2020 IEEE International Conference on Robotics and Automation (ICRA)
31 May - 31 August, 2020. Paris, France

Theoretical Derivation and Realization of Adaptive Grasping Based on Rotational Incipient Slip Detection

Tetsuya Narita, Satoko Nagakari, William Conus, Toshimitsu Tsuboi and Kenichiro Nagasaka

Abstract— **Manipulating objects whose physical properties are unknown remains one of the greatest challenges in robotics. Controlling grasp force is an essential aspect of handling unknown objects without slipping or crushing them. Although extensive research has been carried out on grasp force control, unknown object manipulation is still difficult because conventional approaches assume that object properties (mass, center of gravity, friction coefficient, etc.) are known for grasp force control. One of the approaches to address this issue is incipient slip detection. However, there has been few detailed investigations of robust detection and control of incipient slip on rotational case. This study makes contributions on deriving the theoretical model of incipient slip and proposes a new algorithm to detect incipient slip. Additionally, a novel sensor configuration and a grasp force control algorithm based on the derived theoretical model are proposed. Finally, the proposed algorithm is evaluated by grasping objects with different weights and moments including a fragile pastry (éclair).**

I. INTRODUCTION

Manipulation is an essential skill for robots to perform various tasks instead of, or in cooperation with, humans. In most cases, robots are required to work in unstructured environments, which is one of the greatest challenges faced by many researchers. Manipulation tasks in an unstructured environment usually require a robot to grasp unknown objects, where a grasp model contains unknown parameters i.e., mass, center of gravity, elasticity, friction coefficient, etc. Therefore, a considerable amount of literature has grown around the theme of unknown object grasping using object recognition, tactile sensing, grasping stability and grasp force control. However, the performance of unknown object grasping is limited by difficulties of handling unknown object properties.

In particular, grasping unknown objects without slipping or crushing them requires appropriate grasp force control to balance force and moment according to the force closure theorem. While various grasping approaches based on force closure have been proposed, conventional approaches assume physical models or object properties are known. Therefore, a novel grasping approach that controls grasp force independently of object properties is required to handle unknown objects. Incipient slip detection is one effective solution to solve this problem. Incipient slip is the physical phenomenon observed when only a partial area in the contact area slips [1]. The contact area here represents the area where the robot hand and an object contact each other. When tangential force is applied to an object, the slip area is expanded, and after the slip area expands over the entirety of the contact area, slip occurs. Namely, incipient slip is the transitional phenomenon of slip. In other words, slip between the robot hand and an object can be predicted by detecting incipient slip. Therefore, once grasp force is determined as the minimum force necessary to keep the incipient slip area from expanding, unknown objects can be grasped without slipping and are less likely to be crushed. This is especially effective for grasping fragile objects.

Tetsuya Narita and others are with Sony Corporation, 2-10-1 Osaki, Shinagawa,Tokyo, 141-8610 Japan (email: Tetsuya.A.Narita@sony.com).

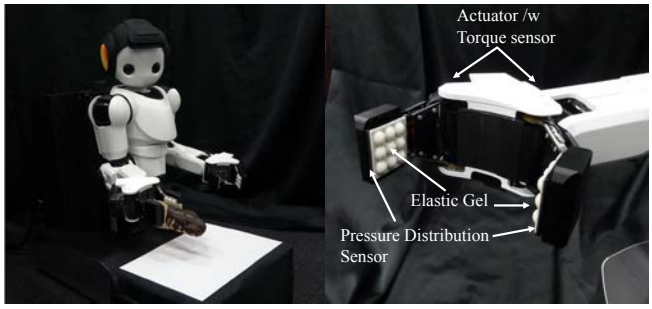

Figure 1. Mobile Manipulator equiped with grippers and sensors to detect rotational incipient slip.

Although various approaches regarding incipient slip detection have been proposed, robust detection and control of incipient slip remain major problems. In particular, no research has been able to detect and control rotational incipient slip for unknown objects. Rotational incipient slip detection is essential for grasping objects subject to a moment of force. There are three fundamental problems faced with incipient slip detection when applied to grasp unknown objects:

A) Physical mechanism of the rotational incipient slip phenomenon is not mathematically well defined.

B) Detection methods of rotational incipient slip and its corresponding sensor configuration have not been established.

C) Robust and general grasp force algorithms to limit rotational incipient slip have not been established.

Contribution

This paper addresses the above three problems and proposes a new algorithm to detect translational and rotational incipient slip, a novel sensor configuration and a grasp force control algorithm.

In summary, the primary contributions of this paper are:

1) Deriving models of translational and rotational incipient slip.

2) A novel sensor configuration and an incipient slip detection algorithm that includes rotation.

3) Grasp force control algorithm that handles incipient slip.

This paper begins by reviewing related research in section II. Section III elucidates the incipient slip mechanism for translational and rotational incipient slip based on the mathematical model. In section IV, conditions for stable and robust detection are clarified and a sensor configuration to detect rotational incipient slip is proposed. Section V discusses the design of a novel grasp force control algorithm to control the area of incipient slip. Section VI demonstrates that proposed algorithm allows a robot to control incipient slip independent of the object properties: mass, friction efficient,

etc., to achieve object grasping that is robust to translational and rotational incipient slip.

II. Related Research

A. Incipient Slip Theory

The incipient slip phenomenon is a behavior based on friction theory that is defined by Amontons' Law. Thus far, much of the current literature on incipient slip pays particular attention to tribology and robot manipulation. Johansson studied mechanisms and perception of incipient slip of human fingers [2][3]. Adams also focused on human fingers and showed a mathematical formulation of elastic friction [4]. Otsuki studied mechanisms of friction for elastic objects and explained incipient slip phenomenon through FEM analysis and experiments [1]. Yamada showed that incipient slip occurs at the edge of the contact area and proved this by using FEM with a human finger model [5]. Maeno [6][7] and Canepa [8] also provide analysis of incipient slip with FEM analysis. Recently, Tada proposed quantification of incipient slip based on elastic contact theory [9]. Although various research has been conducted in the past, such studies remain narrow in focus, dealing only with incipient slip in the translational direction, and has not proposed a mathematical formulation for rotational slip. Cirillo [10] and Melchiorri [11] suggests a detection method of rotational slip using a friction model. However, these proposals assume that model parameters are known and are not applicable for unknown objects.

B. Sensors and Structures

Incipient slip is a subtle and delicate physical phenomenon, hence detection quality is considerably dependent on sensor specification. Early works studying tactile sensing were broadly reviewed in [12]-[14]. Pressure distribution sensors are one of the most widely used tactile sensors. Some have tried to detect slip or incipient slip from distributed force and pressure data [10][15][16]. Vision sensors have been also proposed for incipient slip detection. GelSight is a tactile sensor that captures surface textures using an elastomer and camera [17]. Since the captured data has high spatial resolution information, including surface roughness and texture, deep neural networks are often used to detect incipient slip [18]-[20]. Vibrations and sound signals also provide valuable information for incipient slip detection. Romano used vibrations for touch and slip detection [21]. Teshigawara [22] and Cutkosky [23] distinguished slippage and changes in normal force using vibrations from tactile or force sensors. Although methods using vibrations can be fast and sensitive to subtle changes caused by incipient slip, they are vulnerable to external disturbances. Multimodal methods are one of the proposed answers to these obstacles. BioTac® is a multimodal tactile sensor, consisting of three complementary modalities: force, pressure and temperature. Xu [24] and Su [25] utilized BioTac® for manipulation. Although various sensor types and processing algorithms have been proposed, these proposals are not based on mathematical formulation, which means that essential physical parameters for incipient slip detection is still unclear.

C. Grasp Force Control

Although vast research has been proposed for incipient slip detection, few have highlighted grasp force control. We proposed a grasp force and position controller with incipient slip detection [26]. Maeno proposed a grasp force control method with an elastic finger [27]. Melchiorri calculated forces according to known model [11]. These approaches, however, have failed to verify their effectiveness by grasping unknown or fragile objects and taking rotational incipient slip into account.

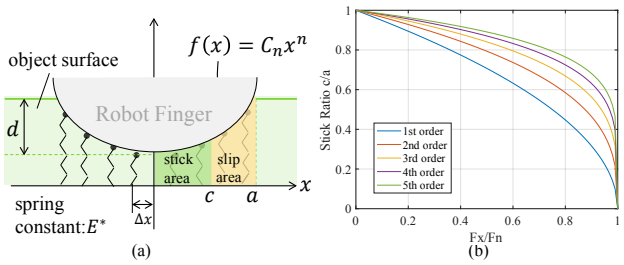

Figure 2. Elastic contact model and plot of the stick ratio. (a) Elastic contact model with hemispheric fingertip and object. (b) Plot of the stick ratio with different orders of contact suface.

III. Incipient Slip Mechanism

In this section, basic incipient slip theory based on elastic contact theory is reviewed and a method to realize robust incipient slip detection is detailed. The incipient slip theory [28] is then extended to rotational slip.

A. Translational Incipient Slip Theory

Fig.2(a) describes the elastic contact model between the robot finger and an object. A contact area of depth *d* is defined between a flat elastic plate with springs and a hemispherical rigid object. The contact surface is described as the function: $f(x) = C_n x^n$, where C_n is a constant and n is the order of the function. The contact area is assumed to include both stick and slip areas. The total normal force F_N, which in this case is equivalent to the grasp force, can be calculated as follows:

$$F_N = 2E^* \int_0^a u_z(x)dx = \frac{2n}{n+1} E^* C_n \lambda_n a^{n+1} \qquad (1)$$

where E^* is effective Young's modulus calculated from $\frac{1}{E^*} = \frac{1-{\nu_1}^2}{E_1} + \frac{1-{\nu_2}^2}{E_2}$, using Yong's moduli of the robot finger E_1 and object E_2 as well as their shear moduli ν_1 and ν_1. $u_z(x)$ is the indentation depth at x. λ_n is a scaling factor that maps from one-dimensional contact to three-dimensional contact with n order contact surface [29].

Tangential force can be calculated based on the elastic contact theory as follows:

$$F_x = 2G^* \int_0^c u_z(x)dx + 2\int_c^a \mu E^* u_z(x)dx$$
$$= \frac{2n}{n+1} \mu E^* C_n \lambda_n a^{n+1} \left\{1 - \left(\frac{c}{a}\right)^{n+1}\right\} \qquad (2)$$

where μ is the friction coefficient and G^* is the transverse elastic modulus. From (1), (2), the following is derived:

$$\frac{c}{a} = \left(1 - \frac{F_x}{\mu F_N}\right)^{\frac{1}{n+1}}. \qquad (3)$$

The left side of (3) represents the ratio of stick area against contact area (stick ratio), in other words, the tendency of incipient slip. Drop of the stick ratio toward zero implies an increased tendency of incipient slip.

Fig.2(b) is a plot of (3), which represents the stick ratio with different orders of contact surface n. Fig.2(b) shows that the stick ratio dropped to zero suddenly when grasp force decreases or tangential force increases. This sudden drop must be avoided for stable grasp control. Also, (3) indicates that the stick ratio is dependent on the unknown parameter, the friction coefficient, which makes it difficult to estimate the stick ratio. These two are the major problems to control incipient slip with unknown parameters and are discussed in section IV.

B. Rotational Incipient Slip Theory

Detection of rotational incipient slip for unknown objects is essential for handling unknown objects where moments are applied. In this section, the translational incipient slip theory is extended to rotational incipient slip.

The total moment around the contact center can be calculated as follows:

$$T_\theta = \int_{-a}^{a} r f_\theta(r) dr = F_N a \mu \left\{ -\frac{n+1}{6n}\left(\frac{c}{a}\right)^2 - \frac{2(n^2-1)}{6n(n+2)}\left(\frac{c}{a}\right)^{n+2} + \frac{n+1}{2(n+2)} \right\} \quad (4)$$

where r is the distance from the contact center, θ denotes the rotational direction around the center of fingertip and $f_\theta(r)$ is the tangential force in the rotational direction applied per unit area. The stick ratio can be represented as follows:

$$\left(\frac{c}{a}\right)^{n+2} + \frac{n+2}{2(n-1)}\left(\frac{c}{a}\right)^2 - \frac{3n}{2(n-1)} + \frac{T_\theta}{F_z a \mu}\frac{3n(n+2)}{n^2-1} = 0. \quad (5)$$

When the contact surface is assumed quadric (n = 2), the stick ratio becomes:

$$\frac{c}{a} = \sqrt{\sqrt{4 - \frac{8T_\theta}{\mu F_z a}} - 1}. \quad (6)$$

IV. Detection Method and Sensor Configuration

A. Incipient Slip Detection Method

According to section III, two major problems need to be addressed to control incipient slip stably: 1) Avoiding sudden stick ratio drop and 2) Calculating or estimating the stick ratio independent of the friction coefficient. In this section, these problems are further discussed.

For problem 1), the relationship between elastic contact surface and the stick ratio is first mathematically analyzed. Fig.3 provides the analytical model and results of different contact surface shapes. The contact surface is composed of a flat surface and a curved surface, where b/a represents the surface ratio. As shown in Fig3, there is a clear trend that the stick ratio drops suddenly when the surface ratio is large. This result gives interesting insight on the incipient slip mechanism. The result implies that when the slip area reaches the flat surface, slip occurs suddenly. In Amonton's friction law, slip behavior is related to static friction and the strength of the normal pressure distribution. Consequently, a sudden drop is considered to occur when the gradient of contact pressure distribution is flat. The above theory for flat and curved contact cases is also confirmed with the ANSYS® simulation software.

The elastic flat plate and elastic curved surface are contacted by a rigid plate. The same tangential force is applied to the rigid plate. The simulation outputs the contact state distribution: "stick" or "slip", and stick ratio is calculated from

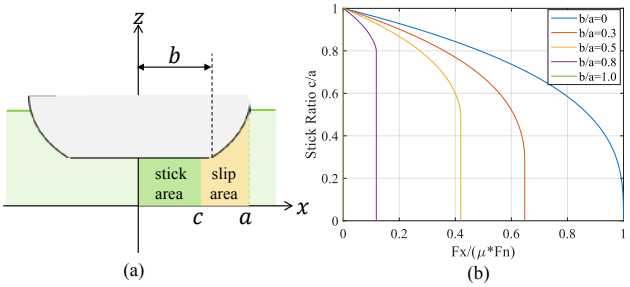

Figure 3. Elastic contact model with flat and curved area. (a) Contact model. (b) Plot of stick ratio with different flat area/curved area ratio.

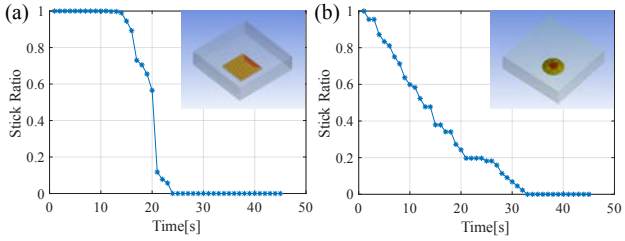

Figure 4. ANSYS® simulation results. Rigid plane is shown as a transparent rectangular shape and elastic contact surface is shown as a colored shape. (a) Plot of stick ratio of contact with elastic flat plane. (b) Plot of stick ratio of contact with elastic sphere.

the state distribution. Fig.4 shows that the stick ratio changes slowly for the curved surface contact, while it drops suddenly for the flat surface contact. These results support the theory that a robot finger with curved surface is preferable for incipient slip control.

For problem 2), a stick ratio estimation method with shear displacement u_x is proposed. Shear displacement represents the displacement of the robot elastic fingertip in the tangential direction when tangential force is applied to the grasped object. If shear displacement of fingertip can be measured, (3) can be rewritten as follows:

$$\frac{c}{a} = (1 - \Psi(\mu, F_N)u_x)^{\frac{1}{n+1}} \quad (7)$$

where $\Psi(\mu, F_N) = \frac{G^*\pi\left(\frac{n+1}{2n}\frac{F_N}{E^* C_n \lambda_n}\right)^{\frac{2}{n+1}}}{\mu F_N}$. Equation (7) shows that if shear displacement u_x is zero, the stick ratio becomes equal to one, which means that incipient slip no longer occurs. Shear displacement can be calculated by tracking the displacement of the maximum pressure point. When there is difficulty in tracing the maximum pressure point due to sensing noise, the Center of Pressure (CoP) is also effective as an approximation of the maximum pressure point.

The same applies for the rotational case. Rotational shear displacement u_θ can be defined as the displacement of the robot elastic fingertip in the rotational direction when torque is applied to the grasped object. Equation (6) can be rewritten with rotational shear displacement as follows:

$$\frac{c}{a} = \sqrt{\sqrt{4 - \Phi(\mu, F_N)u_\theta} - 1} \quad (8)$$

where $\Phi(\mu, F_N) = \frac{16G^*\left(\frac{3}{4E^* C_2 \lambda_2}F_N\right)^{\frac{1}{3}}}{3\mu F_N}$. In the same manner as the translational case, if the rotational shear displacement u_θ can

be controlled to be zero then the stick ratio becomes equal to one for rotational incipient slip. However, rotational shear displacement cannot be detected with the same method as translational slip because rotational incipient slip does not change the maximum pressure point when the robot finger is assumed to be a single hemisphere in Fig.2. To measure the rotational shear displacement with the convex fingertip, a novel sensor configuration is proposed in the following section.

B. Sensor Configuration

In order to measure rotational shear displacement, a finger composed of multiple elastic hemispheres as shown in Fig.5 is proposed. The translational shear displacement at each elastic hemisphere can be measured with the CoP according to the previous section. The translational shear displacement at each elastic hemisphere would change according to the rotational shear displacement. The relationship between rotational and translational shear displacement, before and after rotational incipient slip, can be represented using an affine transform:

$$\begin{pmatrix} x_i' \\ y_i' \\ 1 \end{pmatrix} = \begin{pmatrix} cos\theta & -sin\theta & t_x \\ sin\theta & cos\theta & t_y \\ 0 & 0 & 1 \end{pmatrix} \begin{pmatrix} x_i \\ y_i \\ 1 \end{pmatrix} \tag{9}$$

where i represents the index of the elastic sphere. θ, t_x and t_y represent rotational shear displacement, x-axis, and y-axis translational displacement respectively. In order to solve three unknown parameters: θ, t_x, t_y, more than three equations are needed. In other words, fingertip contacts with at least two hemispheres is necessary to calculate equation (9).

For measuring the CoP, a sensor capable of measuring pressure distribution is required. A capacitive pressure distribution sensor was chosen that calculates pressure by transforming deformation of sensor material to capacity change at each node.

A urethane gel composed of an array of elastic hemispheres is placed on top of the sensor to allow rotational shear displacement estimation. To measure the shear displacement accurately, the distance between each sensor node (sensor pitch) and the number of elastic hemispheres are carefully selected. Fig.6 provides the simulation results on estimation error of translational shear displacement with different amounts of elastic hemispheres and different sensor node pitches. As can be seen in Fig.6, a smaller sensor node pitch is a key factor for lower estimation error. From a practical point of view, however, node pitch should be carefully decided because of a trade-off between smaller node pitch and larger processing cost or lower sensitivity. To keep a high enough data sampling frequency and sensitivity, a sensor node pitch of 3mm is chosen. The data sampling frequency is 100Hz. Fig.6 also shows that the hemisphere array configuration also affects estimation error. With more hemispheres used, the estimation error is partially reduced except the case with more than 3x3 hemispheres used. This result is explained by the fact that less sensor nodes are assigned for each hemisphere with more hemispheres used. In order to minimize the error, 3 x 3 hemisphere configuration is selected. Considering the small size requirement, the fingertip size is decided as 40x40mm and 11x13 pressure sensor nodes are implemented.

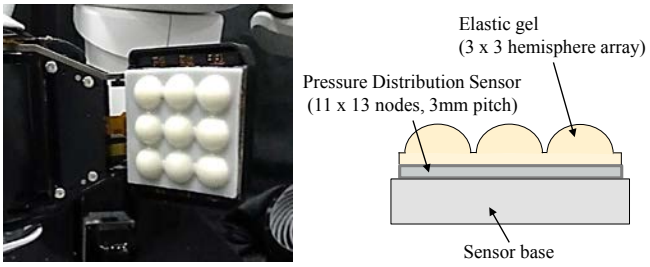

Figure 5. Proposed elastic finger tip (left) and cross-section (right).

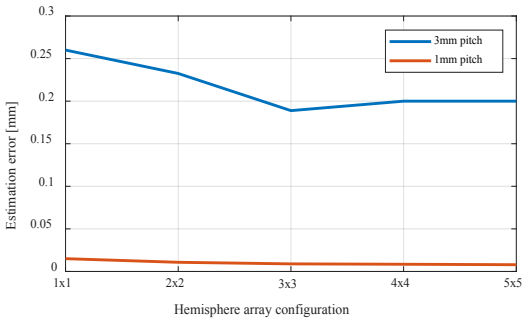

Figure 6. Simulated translational shear displacement estimation error for different fingertip gel hemisphere array configurations when the sensor node pitch is 1mm and 3mm.

In particular, no shear displacement means no slippage occurs between the finger and the objects. Additionally, this allows robots to grasp objects without slippage. The next section moves on to discuss a grasp force control algorithm to prevent shear displacement.

V. Grasp Force Control Algorithm

In order to prevent shear displacement for object grasping, the shear displacement should be controllable by grasp force. This section first gives theoretical explanations that the shear displacement can be controlled by grasp force and then proposes a grasp force control algorithm.

The proposed grasp force algorithm is based on the elastic contact theory of the same mechanical model shown in Fig.2. Under the precondition that the robot finger is an elastic convex shape and is deformed by normal force, the contact area is considered to be a circle whose radius is a. The radius of the contact area is represented as a function of grasp force:

$$a = \left(\frac{n+1}{2n}\frac{F_N}{E^* C_n \lambda_n}\right)^{\frac{1}{n+1}}. \tag{10}$$

Assuming the tangential force applied to the elastic fingertip is constant, then the shear force F_x of the elastic fingertip can be represented as follows:

$$F_x = \int_{-a}^{a} G^* u_x \, dr = 2G^* u_x a. \tag{11}$$

The relationship between translational shear displacement u_x and grasp force F_N is derived from (10) and (11):

$$u_x = \frac{F_x}{G^*\left(\frac{n+1}{2n}\frac{F_N}{E^* C_n \lambda_n}\right)^{\frac{1}{n+1}}}. \tag{12}$$

From (4), the moment T_θ of the elastic fingertip is:

$$T_\theta = \int_{-a}^{a} G^* \frac{r}{a} u_\theta \, r dr = \frac{2}{3} G^* u_\theta a^2. \tag{13}$$

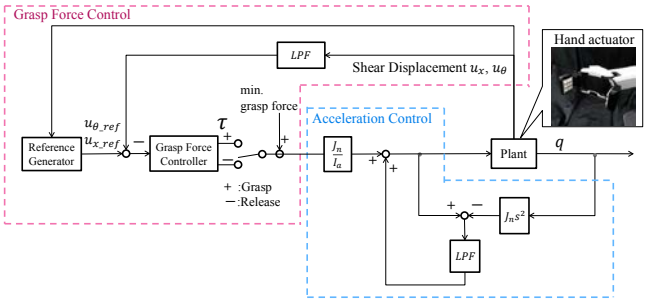

Figure 7. Proposed grasp force controller for a finger.

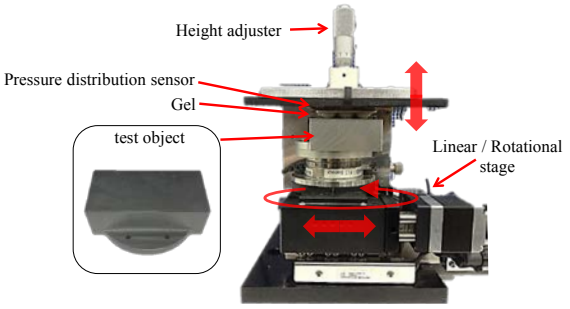

Figure 8. Experimental setup to evaluate shear displacement estimation accuracy. Linear and rotational displacement are controlled by a 2 axis positioning stage. Contact force is controlled with the height adjuster.

The relationship between rotational shear displacement u_θ and grasp force F_N is derived from (10) and (13):

$$u_\theta = \frac{3T_\theta}{2G^*\left(\frac{n+1}{2n}\frac{F_N}{E^* C_n \lambda_n}\right)^{\frac{2}{n+1}}}. \quad (14)$$

Equations (12) and (14) show that the translational and rotational shear displacement are defined as functions of grasp force (F_N), which suggests that displacement can be controlled by grasp force. It should be noted that these theories are only applied to convex elastic fingertips.

Fig.7 shows the proposed grasp force control algorithm. This algorithm is composed of two control blocks: Grasp Force Control and Acceleration Control block. The grasp Force Control block calculates grasp force at 1kHz so that no translational or rotational shear displacement occurs. Since translational and rotational incipient slip generally occur simultaneously, grasp force for translational and rotational incipient slip are first calculated respectively and then summed. A first order of low pass filter is used to suppress the noise of shear displacement values. The reference generator updates the target shear displacement dependent on grasp status and application. Since two contact points between an object and hemispheres on the finger is necessary to calculate shear displacement from the result in section IV, minimum grasp force is added to keep contact. The minimum contact force is determined as the grasp force applied when two contact points are detected for the first time. The acceleration Control block controls the acceleration of the actuators used to generate accurate grasp force at 8kHz. A disturbance observer (DOB) is adopted to cancel disturbance noise caused by inertia and friction in an actuator, where J_n is nominal inertia of the actuator, I_a is target inertia and plant is described as a second order system. A first order of low pass filter is used in the DOB.

It is interesting to note that the proposed algorithm can be extended to other manipulation tasks such as object release (i.e., hand-over or placement on a table). For example, grasp force is expected to decrease when a robot hands over an object to human. The shear displacement, in this case, would change as the human begins to support the object against gravity. The opposite is true when grasping objects. This extension is simply realized by switching the increase and decrease of grasp force (Fig.7) with the same incipient slip detection and force control algorithm. Although this is simple extension, smooth object release motion is achieved.

VI. Evaluation

A. Experimental Setup and Procedure

In order to evaluate the proposed method, two different experiments are conducted. Since the proposed incipient slip detection method detects incipient slip based on shear displacement, the estimation accuracy of shear displacement is firstly evaluated. For this evaluation, a 2-axis (rotational and translational) position control stage (Fig.8) is utilized. The proposed elastic fingertip and a test object are in contact with each other, and contact force is maintained by adjusting the stage's height. Shear displacement is applied to the object by position control of the stage and the position is measured by the embedded encoder. Shear displacement is calculated using CoP as an approximation of the maximum pressure point as described in section IV-B. The accuracy is evaluated by comparing the encoder position and estimated shear displacement derived from (9).

Secondly, the proposed grasp force control algorithm is evaluated using a mobile manipulator equipped with two 7 DoF arms and parallel link grippers composed of the proposed tactile sensor and torque-controlled actuators (Fig.1). The experiments are conducted in the following order. First, the gripper grasps a target object placed on a flat plane. Second, the object is lifted by the arm. Third, the grasped object is held in the air for 4 seconds. Finally, the object is placed at its original position. Grasp force is determined using the proposed algorithm with no object information given to the robot. Every experiment is conducted using this test sequence. In each test sequence, grasp force τ derived from the proposed algorithm, shear displacement u_x and u_θ from Fig.7 are recorded at 10 Hz. Fig.12 shows 3 different test objects used in this evaluation.

B. Estimation Accuracy of Shear Displacement

Fig.9 provides the results of shear displacement estimation accuracy. The horizontal axis represents the applied displacement, which was measured using the stage encoder, and the vertical axis represents estimated shear displacement. R^2 represents the coefficient of determination of the linear regression line. Although the estimation error is observed at 15% and 3% for translational and rotational displacement respectively, the estimated displacement shows strong linear correlation with the applied displacement. A possible cause of error is the approximation error of CoP.

C. Robustness of Proposed Grasp Force Control Algorithm to Object Weight and Moment Variations

At the first step of the evaluation, grasp force τ, shear displacement u_x and u_θ, are observed. A rectangular plastic bottle is utilized as a target object. As shown in Fig.10-a, grasp force is controlled according to the values of u_x and u_θ.

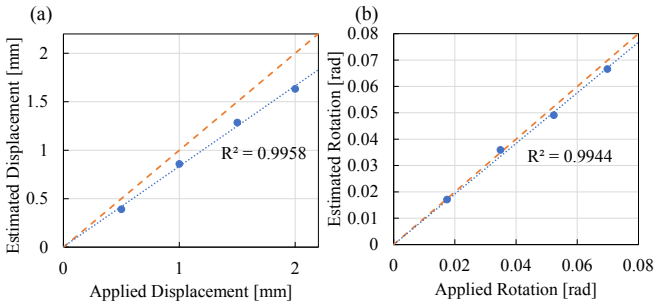

Figure 9. Estimation accuracy of (a) translational shear displacement and (b) rotational shear displacement. The difference between the orange dotted line and the blue plots represents the estimation error.

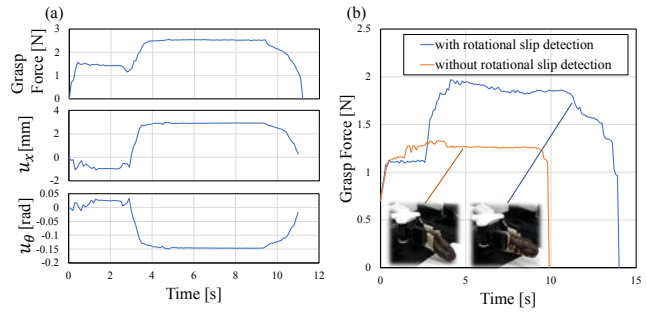

Figure 10. (a) Grasp force τ, shear displacement u_x and u_θ when grasping the rectangular plactic bottle, (b) Grasp force with and without rotational slip detection when grasping an éclair.

The observation shows that the grasp force drastically increases and decreases during the whole sequence. Since these changes can be observed at the exact time of lifting and placing the object, it appears that the proposed algorithm detects force and moment change adaptively by measuring incipient slip.

In order to further confirm the robustness of the proposed algorithm, grasp force, derived from the proposed algorithm, is measured with an object of varied weights and moments. In this evaluation, the derived grasp force τ is compared with minimum grasp force (τ_{min}) to evaluate that the grasp force is not larger than necessary. τ_{min} is investigated beforehand by conducting grasp trials repeatedly given constant grasp forces. τ_{min} is selected as the minimum grasp force among successful trials. A rectangular plastic bottle (Fig.12-1,2) is used for this evaluation. Object weight is changed by adjusting the amount of small pieces of metal in the bottle and object moment is changed by grasping at different positions on the bottle. Fig.11 provides results of this experiment. Since grasp force τ is stably close to τ_{min}, it is demonstrated that the proposed algorithm derives the minimum necessary grasp force, adaptively and robustly with different weight and moment.

Finally, the grasp success rate is investigated for each object to evaluate effectiveness of the proposed algorithm. The success rate is derived from 10 trials for each object. If an object does not touch the ground during a test sequence, the trial is considered a success. The results of all target objects are summarized in Table I. As Table I shows, every target object, including a fragile pastry, can be grasped without fail independent of object shape, weight, moment and stiffness. In order to investigate effectiveness of rotational incipient slip detection, grasp force is compared with and without rotational incipient slip detection, which is illustrated in Fig.10-b. The comparison reveals that the grasp force is not enough in no rotational slip detection case. In addition, the results also show that rotational slip detection is essential for grasping objects with unknown object properties.

VII. Conclusion and Future Work

This paper derived the rotational incipient slip theory by expanding from the translational case and also clarified essential conditions to stably detect and control incipient slip. This theoretically contribution led to the proposal of a novel incipient slip detection method, sensor configuration and adaptive grasp force control algorithm. The experimental results show that the proposed algorithm is able to adaptively calculate grasp force for unknown objects with varied weights, moments and stiffnesses. Finally, grasping objects, including fragile pastries, was realized without slipping or crushing them.

Future direction of our work includes improvement of the sensing ability and control algorithm. Robustness and durability of the sensor structure is an essential aspect from a practical perspective. Increasing spatial resolution is also an important future work. In addition, further investigation of grasp control algorithm is needed for different hand configurations such as a multi-fingered hand. Since graspable objects range is limited due to geometric constraints of parallel grippers, a multi-fingered hand may be one of the possible options.

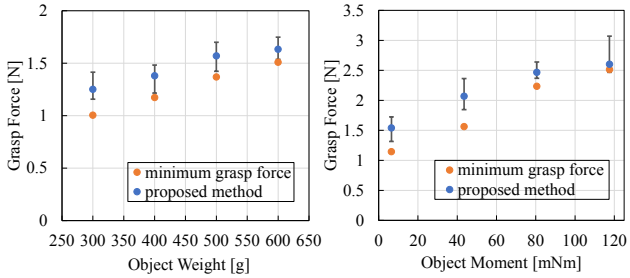

Figure 11. Comparison between grasp force τ derived by proposed method and minimum grasp force τ_{min} with different weight and moment. The range and mean of grasp force τ during 10 grasp trials is represented.

TABLE I. Specification of the Test Objects

	Object	*Object Properties*		*Success Rate*
		Mass [g]	*Moment* [mNm]	
1	Plastic bottle (placed vertically)	600	0	10/10
2	Plastic bottle (placed horizontally)	251	120	10/10
3	Eclair	104	39	10/10

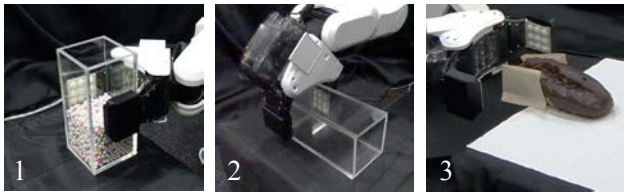

Figure 12. The 3 test objects. The robot grasps objects at the orientation shown in the picture.

REFERENCES

[1] M. Otsuki and H. Matsukawa, "Systematic breakdown of Amontons' law of friction for an elastic object locally obeying Amontons' law," *Scientific reports*, 2013, 3: 1586

[2] R.S.Johansson and G. Westling, "Signals in tactile afferents from the fingers eliciting adaptive motor responses during precision grip," *Experimental brain research*, 1987, 66.1: 141-154.

[3] R.S.Johansson and G. Westling, "Roles of glabrous skin receptors and sensorimotor memory in automatic control of precision grip when lifting rougher or more slippery objects," *Experimental brain research*, 1984, 56.3: 550-564.

[4] M.J.Adams, S. A. Johnson, P. Lefevre, V. Levesque, V. Hayward, T. Andre and J. L. Thonnard, "Finger pad friction and its role in grip and touch," *Journal of The Royal Society Interface,* 2013, 10.80: 20120467.

[5] D. Yamada, T. Maeno and Y. Yamada, "Artificial finger skin having ridges and distributed tactile sensors used for grasp force control," in *Proc. 2001 IEEE/RSJ International Conference on Intelligent Robots and Systems.* Expanding the Societal Role of Robotics in the the Next Millennium (Cat. No. 01CH37180). IEEE, 2001. p. 686-691.

[6] T. Maeno, K. Kobayashi and N. Yamazaki, "Relationship between structure of finger tissue and location of tactile receptors," *Nippon Kikai Gakkai Ronbunshu, C Hen/Transactions of the Japan Society of Mechanical Engineers,* Part C, 1997, 63.607: 881-888.

[7] T. Maeno, T. Kawai and K. Kobayashi, "Analysis and design of a tactile sensor detecting strain distribution inside an elastic finger," in *Proc. 1998 IEEE/RSJ International Conference on Intelligent Robots and Systems*. Innovations in Theory, Practice and Applications (Cat. No. 98CH36190). IEEE, 1998. p. 1658-1663.

[8] G. Canepa, R. Petrigliano, M. Campanella and D. D. Rossi, "Detection of incipient object slippage by skin-like sensing and neural network processing," *IEEE Transactions on Systems, Man, and Cybernetics,* Part B (Cybernetics), 1998, 28.3: 348-356.

[9] M. Tada, T. Shibata, and T. Ogasawara, "Investigation of the touch processing model in human grasping based on the stick ratio within a fingertip contact interface," in *Proc. IEEE Int. Conf. Systems, Man and Cybernetics*, tp1n4, 2002.

[10] A. Cirillo, P. Cirillo, G. D. Maria and C. Natale, "Control of linear and rotational slippage based on six-axis force/tactile sensor," *2017 IEEE International Conference on Robotics and Automation (ICRA)*. IEEE, 2017. p. 1587-1594.

[11] C. Melchiorri, "Slip detection and control using tactile and force sensors," *IEEE/ASME transactions on mechatronics*, 2000, 5.3: 235-243.

[12] Z. Kappassov, J. A. Corrales and V. Perdereau, "Tactile sensing in dexterous robot hands," *Robotics and Autonomous Systems*, 2015, 74: 195-220.

[13] M.T.Francomano, D. Accoto and E. Guglielmelli, "Artificial sense of slip—A review," *IEEE Sensors Journal*, 2013, 13.7: 2489-2498.

[14] R. S. Dahiya, G. Metta, M. Valle and G. Sandini, "Tactile sensing—from humans to humanoids," *IEEE transactions on robotics*, 2009, 26.1: 1-20.

[15] D. Cockburn, J. Roberge, T. Le, A. Maslyczyk and V. Duchaine, "Grasp stability assessment through unsupervised feature learning of tactile images," *2017 IEEE International Conference on Robotics and Automation (ICRA)*. IEEE, 2017. p. 2238-2244.

[16] T. P. Tomo, A. Schmitz, W. K. Wong, H. Kristanto, S. Somlor, J. Hwang, L. Jamone and S. Sugano, "Covering a robot fingertip with uSkin: A soft electronic skin with distributed 3-axis force sensitive elements for robot hands," *IEEE Robotics and Automation Letters*, 2017, 3.1: 124-131.

[17] W.Yuan, R. Li, M. A. Srinivasan and E. H. Adelson. "Measurement of shear and slip with a GelSight tactile sensor," *2015 IEEE International Conference on Robotics and Automation (ICRA)*. IEEE, 2015. p. 304-311.

[18] R. Calandra, A. Owens and D. Jayaraman. "More than a feeling: Learning to grasp and regrasp using vision and touch," *IEEE Robotics and Automation Letters*, 2018, 3.4: 3300-3307.

[19] J. Li, S. Dong and E. Adelson. "Slip detection with combined tactile and visual information," *2018 IEEE International Conference on Robotics and Automation (ICRA)*. IEEE, 2018. p. 7772-7777

[20] S. Stepputtis, Y. Yang and H. B. Amor, "Extrinsic Dexterity Through Active Slip Control Using Deep Predictive Models," *2018 IEEE International Conference on Robotics and Automation (ICRA)*. IEEE, 2018. p. 3180-3185.

[21] J. M. Romano, K. Hsiao, G. Niemeyer, S Chitta and K. J. Kuchenbecker, "Human-inspired robotic grasp control with tactile sensing," *IEEE Transactions on Robotics*, 2011, 27.6: 1067-1079.

[22] S. Teshigawara, T. Tsutsumi, S. Shimizu, Y. Suzuki, A. Ming, M. Ishikawa and M. Shimojo, "Highly sensitive sensor for detection of initial slip and its application in a multi-fingered robot hand," *2011 IEEE International Conference on Robotics and Automation*. IEEE, 2011. p. 1097-1102.

[23] M. R. Tremblay and M. Cutkosky, "Estimating friction using incipient slip sensing during a manipulation task," in *Proc. IEEE International Conference on Robotics and Automation. IEEE*, 1993. p. 429-434.

[24] D. Xu, G. E. Loeb and J. A. Fishel, "Tactile identification of objects using Bayesian exploration," *2013 IEEE International Conference on Robotics and Automation*. IEEE, 2013. p. 3056-3061.

[25] Z. Su, K. Hausman, Y. Chebotar, A. Molchanov, G. E. Loeb, G. S. Sukhatme and S. Schaal, "Force estimation and slip detection/classification for grip control using a biomimetic tactile sensor," *2015 IEEE-RAS 15th International Conference on Humanoid Robots (Humanoids)*. IEEE, 2015. p. 297-303.

[26] T. Takahashi, T. Tsuboi, T. Kishida, Y. Kawanami, S. Shimizu, M. Iribe, T. Fukushima and M. Fujita, "Adaptive grasping by multi fingered hand with tactile sensor based on robust force and position control," *2008 IEEE International Conference on Robotics and Automation*. IEEE, 2008. p. 264-271.

[27] T. Maeno. S. Hiromitsu and T. Kawai, "Control of grasping force by detecting stick/slip distribution at the curved surface of an elastic finger," in *Proc. 2000 ICRA Millennium Conference. IEEE International Conference on Robotics and Automation. Symposia Proceedings (Cat. No. 00CH37065)*. IEEE, 2000. p. 3895-3900.

[28] P. Valentin, "Basic ideas and applications of the method of reduction of dimensionality in contact mechanics," *Physical Mesomechanics. 15. 254-263. 10.1134/S1029959912030022, 2012*

[29] G. Thomas and P. Valentin, "Mapping of three-dimensional contact problems into one dimension," *Physical review. E, Statistical, nonlinear, and soft matter physics. 76. 036710. 10.1103/PhysRevE.76.036710, 2007.*